

AperTO - Archivio Istituzionale Open Access dell'Università di Torino

Elucidating the structure and dynamics of CO ad-layers on MgO surfaces

This is the author's manuscript

Original Citation:

Availability:

This version is available <http://hdl.handle.net/2318/1746085> since 2020-07-27T16:52:35Z

Published version:

DOI:10.1039/c9cp05418a

Terms of use:

Open Access

Anyone can freely access the full text of works made available as "Open Access". Works made available under a Creative Commons license can be used according to the terms and conditions of said license. Use of all other works requires consent of the right holder (author or publisher) if not exempted from copyright protection by the applicable law.

(Article begins on next page)

Elucidating the structure and dynamics of CO ad-layers on MgO surfaces

Jefferson Maul, Giuseppe Spoto, Lorenzo Mino * and Alessandro Erba *

The combination of quantum-mechanical simulations and infrared absorption spectroscopy measurements provides a clear picture for a long standing puzzle in surface science: the actual structure and vibrational dynamics of the low-temperature ordered CO monolayer adsorbed on (001) MgO surfaces. The equilibrium structure of the commensurate (4×2) adsorbed phase consists of three CO molecules per primitive cell (surface coverage of 75%) located at two inequivalent sites: one molecule seats upright on top of a Mg site while two molecules, tilted off the normal to the surface, are symmetrically positioned relative to the upright one with anti-parallel projections on the surface. This configuration, long believed to be incompatible with measured polarization infrared spectra, is shown to reproduce all observed spectral features, including a new, unexpected one: the vanishing anharmonicity of CO stretching modes in the monolayer.

The accurate description of the chemical or physical adsorption of molecules on surfaces still poses several challenges to state-of-the-art theoretical approaches as: (i) a balanced description of all chemical interactions (including weak dispersive ones) is often required; (ii) the actual structure of the surface and therefore of the adsorption sites is seldom known, which makes the direct comparison with experimental data difficult and often not conclusive; (iii) structural models tend to grow in size very quickly with the complexity of the system thus making the corresponding calculations quite computationally demanding even when periodic-boundary conditions are used instead of a cluster approach.

In this context, the adsorption of CO molecules on the (001) surface of solid MgO is one of the most studied processes as it is considered the prototype of physisorption on a well-defined surface. This system has been extensively studied both experimentally and theoretically to benchmark different methodologies.

Dipartimento di Chimica, Università di Torino, via Giuria 7, 10125, Torino, Italy.

E-mail: lorenzo.mino@unito.it, alessandro.erba@unito.it

† Electronic supplementary information (ESI) available: Effect of the degree of surface coverage on the structure and dynamics of the CO monolayer on MgO(001) surfaces. See DOI: 10.1039/c9cp05418a

In particular, great care has been taken in the characterization of the CO binding energy and vibrational frequency shift upon adsorption, in the low-coverage regime.¹⁻¹⁴

Despite its seemingly simple nature, the physisorption of CO molecules on the clean (001) MgO surface is a complex process whose structural and dynamical features are still far from being fully characterized, particularly so in the low-temperature, high-coverage regime. Low energy electron diffraction (LEED) experiments first showed that, at low temperature ($T \approx 40$ K), the adsorbed molecules form an ordered monolayer whose periodicity is given by a commensurate (4×2) 2D lattice with three CO molecules per primitive cell and six CO molecules per conventional cell (*i.e.*, corresponding to a surface coverage degree of $\gamma = 0.75$).¹⁵ A helium atom scattering (HAS) experiment confirmed the occurrence of the $c(4 \times 2)$ phase and, through the analysis of the relative intensity of two Einstein modes, suggested that the three CO molecules in the primitive cell would be adsorbed on two inequivalent sites.¹⁶ A polarization infrared spectroscopy (PIRS) study shed further light on the low-temperature structure of the CO monolayer: the presence of three peaks with p-polarization (*i.e.*, normal to the surface, γ) and one peak with s-polarization (*i.e.*, parallel to the surface, δ) suggested that one CO molecule would be adsorbed upright while the other two would be adsorbed at two energetically equivalent sites and would be tilted with antiparallel projections on the surface.¹⁷

The actual geometry of the CO monolayer on the (001) MgO surface at low temperature has been the subject of extensive theoretical work and yet a definitive picture is still to be reached. Adsorption sites and orientations of the CO molecules in the $c(4 \times 2)$ phase were first investigated by use of semi-empirical potentials.¹⁸ Several configurations were reported with different numbers of independent adsorption sites. The most stable one (labeled as E_0) was characterized by two distinct sites with one molecule lying almost flat above a bridge site between two neighboring Mg atoms at the surface, and two molecules lying close to two adjacent Mg sites and slightly tilted with respect to the normal to the surface, with anti-parallel projections on the surface. The second most stable configuration (labeled P_0) exhibits three

distinct adsorption sites with one CO perpendicular to the surface, one slightly tilted and one almost parallel to the surface bridging two Mg atoms, and is therefore incompatible with the PIRS experimental fingerprint. Their least stable configuration (labeled H_0) is characterized by two independent adsorption sites, where one molecule seats upright on top of a Mg site while the two non-perpendicular molecules are symmetrically positioned relative to the upright one. Periodic Hartree-Fock calculations reported the P_0 and H_0 configurations to be energetically equivalent and overall more stable than E_0 .¹⁹ A dynamical model based on semi-empirical potentials concluded that E_0 should be regarded as the most convenient configuration for the low-temperature $c(4 \times 2)$ phase.²⁰ A Monte Carlo simulation based on empirical pair-wise potentials reported that the most stable low-temperature configuration for the CO monolayer on the (001) MgO surface should rather be the H_0 one.²¹ Finally, semi-empirical potential calculations combined with neutron diffraction suggested that the observed structure of the system should be regarded as a mixture of E_0 , H_0 and P_0 configurations.²²

In the present study, we investigate the structure of the low-temperature $c(4 \times 2)$ phase of the CO monolayer on the (001) MgO surface by means of full structural relaxations within quantum-mechanical calculations based on the density functional theory and we find the H_0 configuration to be the most stable one. Based on configurational considerations and on semi-empirical potential calculations, the H_0 structure has long been considered to be incompatible with the observed PIRS fingerprint.¹⁸ Here, we compute quantum-mechanically the infrared spectrum of the equilibrium structure, we compare to previously and newly measured experimental infrared spectra, and we show instead that all measured spectral features are reproduced by the H_0 configuration.

Furthermore, from the newly recorded infrared spectra, an unexpected spectral feature emerges: the infrared peak

corresponding to the first overtone of the in-phase stretching of all CO molecules is recorded at a frequency that is exactly twice as large as that of the corresponding fundamental transition,

thus indicating a vanishing anharmonicity in the vibrational potential of the adsorbed CO molecules in the ordered monolayer. The application of a recently developed quantum-mechanical scheme^{23,24} for the calculation of anharmonic vibrational states through the description of high-order terms of the potential energy surface (PES) and phonon-phonon couplings allows to show that the optimized H_0 structural model indeed imparts a vanishing anharmonicity to the nuclear potential of the adsorbed monolayer.

Quantum-mechanical calculations are performed within the density functional theory (DFT) with the hybrid B3LYP exchange-correlation functional, as implemented in the Crystal program.²⁵⁻²⁷ All-electron triple-zeta quality basis sets are used for the MgO substrate²⁸ and CO molecules.²⁹ The MgO surface is modeled as a three-layer slab. Convergence of all relevant quantities with respect to the thickness of the substrate has been checked against a five-layer slab model. The convergence in energy of each self-consistent field process is set to 10^{-10} Ha for all geometry optimizations and harmonic frequency calculations. Reciprocal space is sampled on a 3×3 mesh of points for the $c(4 \times 2)$ model.

The Fourier-transform infrared (FTIR) spectra were recorded using a Bruker Equinox 55 FTIR spectrometer, equipped with an MCT cryogenic detector, with the sample compartment modified to accommodate a Oxford CCC 1204 cryostat allowing the study of species adsorbed in controlled temperature (between 300 and 14 K) and pressure conditions.^{30,31} The investigated sample is a MgO "smoke" sample constituted by nearly perfect cubelets, which can be compared with the results obtained on the (001) surfaces of single crystals.⁸ The advantage of using powders instead of single crystals is the higher specific surface area of the samples ($\approx 10 \text{ m}^2 \text{ g}^{-1}$), which ensures higher spectral quality, also allowing for the observation of CO overtone modes.

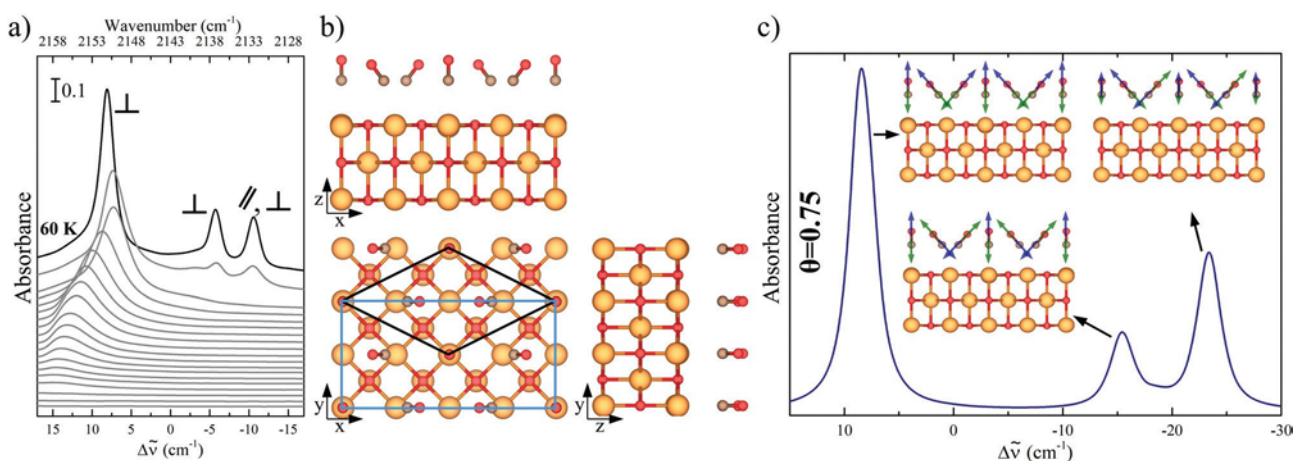


Fig. 1 Structural and spectroscopic characterization of the low-temperature CO monolayer on (001) MgO surfaces: (a) experimental FTIR spectra, recorded at 60 K, of CO adsorbed at increasing coverages on MgO (the spectra have been vertically offset for clarity). The peaks are labeled based on their polarization ($>$ and/or \parallel) as determined in previous studies using PIRS;¹⁷ (b) top and side views of the equilibrium configuration obtained from full quantum-mechanical structural relaxations performed with the B3LYP hybrid functional of the DFT; (c) simulated infrared spectrum from quantum-mechanical calculations and graphical representation of the normal modes of vibration associated to the three intense peaks (arrows of the same color correspond to in-phase atomic motions). In the spectra, $\Delta\tilde{\nu}$ is the frequency shift with respect to the CO stretching in gas phase.

Results on the structure and vibrational dynamics of the low-temperature CO monolayer adsorbed on (001) MgO surfaces are summarized in Fig. 1. Panel (a) reports the experimental infrared spectra recorded at 60 K at different CO coverages, plotted as a function of the frequency shift $\Delta\nu$ with respect to the CO stretching in gas phase (*i.e.*, 2143 cm^{-1}). At low CO coverage, only one intense spectral feature is observed whereas at higher coverage three intense spectral features appear that match those originally reported to occur below 45 K by Heidberg *et al.*¹⁷ The most intense peak is blue-shifted with respect to gas phase CO while the two new peaks are red-shifted. From PIRS experiments, the three peaks are observed with p-polarization while only the third one is observed when s-polarization is used, thus indicating also a change in the dipole parallel to the surface in the latter case.¹⁷ Panel (b) of Fig. 1 shows top and side views of the equilibrium low-temperature structure of the $c(4 \times 2)$ phase obtained from the quantum-mechanical calculations. A 2D slab model has been set up, with three layers in the MgO substrate and with six adsorbed CO molecules in the conventional (4×2) cell with no symmetry constraints whatsoever. A full geometry optimization has been performed where all structural degrees of freedom were free to relax (atomic positions and lattice parameters). A quasi-Newton algorithm for energy minimization has been used,³² based on the analytical evaluation of energy and forces at each explored nuclear configuration, as combined with a Broyden-Fletcher-Goldfarb-Shanno scheme for updating the Hessian. Tight convergence criteria on both forces and atomic displacements were used. Different initial adsorption sites and orientations of the six CO molecules have been explored, which all resulted in the same final optimized structure (given in Fig. 1). Despite no symmetry constraints were imposed, the six CO molecules in the optimized structure are symmetry equivalent by two in the (4×2) cell (shown in blue in the top view). As a consequence, the optimized structure can be defined in terms of a smaller primitive cell containing only three CO molecules (shown in black in the top view). Inspection of the two side views of the equilibrium structure shows how the axes of all the CO molecules lie in xz planes, with zero projections along y . The equilibrium structure of the CO monolayer is characterized by one upright CO molecule adsorbed on top of a Mg atom, and by two tilted CO molecules adsorbed on two energetically equivalent sites, slightly displaced from the top of two Mg atoms, symmetrically distributed with respect to the upright one, and with anti-parallel projections on the surface. The equilibrium low-temperature structure found from the present quantum-mechanical calculations therefore coincides with the H_0 nuclear configuration discussed above.

A true equilibrium chemical structure must be a minimum of the PES and therefore the Hessian matrix of energy second derivatives with respect to geometrical parameters must be positive definite (*i.e.*, all eigenvalues must be positive). We have computed the Hessian matrix from numerical derivatives of analytical forces evaluated at displaced atomic configurations. A two-sided finite difference formula has been used to ensure a higher numerical stability. The calculation, run in parallel over

80 cores, took 27 days. When mass-weighted and diagonalized, the Hessian matrix provides the harmonic vibration frequencies and normal modes. All of the 180 computed frequencies are positive (the smallest being of just 5.5 cm^{-1}), thus confirming the nature of equilibrium chemical structure of the optimized nuclear configuration to an unprecedented level of numerical accuracy.

The computed infrared spectrum in the region of the CO stretching modes is reported in Fig. 1(c) as a function of the frequency shift $\Delta\nu$ with respect to the computed harmonic frequency of gas phase CO. All spectral features of the experimental spectra in Fig. 1(a) are qualitatively reproduced by the quantum-mechanical calculations, including the high intensity of the central peak that was reported to be vanishingly small for the H_0 configuration based on semi-empirical potential calculations.¹⁸ In the inset of Fig. 1(c), we sketch the normal modes of vibration corresponding to the three intense peaks and show how they are fully compatible with the results from previous PIRS measurements¹⁷ (arrows of the same color correspond to in-phase atomic motions; the length of the arrows is proportional to the amplitude of the corresponding atomic motion). The most intense peak corresponds to the in-phase stretching of all CO molecules in the monolayer. Due to the symmetry in the orientation of the two tilted molecules with antiparallel projections on the surface, this motion produces a change in the dipole only perpendicularly to the surface and is therefore detected only when p-polarization is used. In the central peak, upright and tilted molecules are stretched out-of-phase. As for the previous motion, there is no change in dipole parallel to the surface while the dipole changes normal to the surface due to the difference in the amplitude of the stretching motion of the upright *versus* tilted CO molecules (therefore this mode is less intense than the first one). The third peak is the only one where the two tilted CO molecules are stretched out-of-phase with respect to one another. This produces a change in the dipole parallel to the surface and indeed this is the only peak detected when s-polarization is used. This peak has also a perpendicular component due to the small (but not null) amplitude of the stretching motion of the upright molecules.

Some aspects of the effect of a different degree of surface coverage and/or of a different periodicity of the monolayer on the structure and dynamics of the system are discussed in the ESI.†

Now, let us discuss a new, unexpected feature of the vibrational spectrum of CO adsorbed on (001) MgO surfaces: the vanishing anharmonicity of the CO stretching vibration in the monolayer. The CO molecule in gas phase is known to exhibit a significant degree of anharmonicity in its stretching motion,³³ the fundamental transition occurring at a frequency $\nu^{0-1} = 2143\text{ cm}^{-1}$ and the corresponding first overtone at a frequency $\nu^{0-2} = 4259\text{ cm}^{-1}$. This corresponds to an anharmonic coefficient $w_a = 2\nu^{0-1} - \nu^{0-2}$ of 26 cm^{-1} . In Fig. 2, we show measured FTIR spectra for CO physisorption on (001) MgO surfaces, recorded at 60 K, as a function of coverage, as in Fig. 1(a). The figure covers the spectral region of the fundamental transition for the in-phase stretching motion of all CO molecules (right panel) and of the corresponding first overtone (left panel). The overtone occurs at a

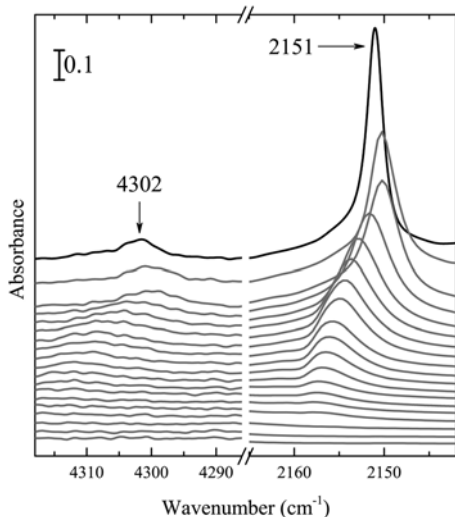


Fig. 2 Experimental FTIR spectra of CO molecules adsorbed on (001) MgO surfaces, recorded at 60 K, as a function of surface coverage (spectra are vertically offset for clarity) in the spectral region of the fundamental transition for the in-phase stretching motion of all CO molecules (right panel) and of the corresponding first overtone (left panel). The overtone $\nu = 2$ occurs at a frequency, ν^{0-2} , that is twice as large as that, ν^{0-1} , of the fundamental transition, as would occur in a perfectly harmonic potential.

frequency, $\nu^{0-2} = 4302 \text{ cm}^{-1}$, that is exactly twice as large as that of the fundamental transition, $\nu^{0-1} = 2151 \text{ cm}^{-1}$, thus yielding a null anharmonic coefficient $w_a = 0$, as would occur in a perfectly harmonic potential.

Quantum-mechanical calculations confirm this feature and provide further insight on its origin. We have applied a scheme for the evaluation of cubic and quartic terms of the PES and for the numerical solution of the vibrational Schrödinger equation for an anharmonic potential (namely, the vibrational configuration interaction method, VCI), as recently implemented in the Crystal program.^{23,24} First, we studied the anharmonicity of the stretching mode in the CO molecule in gas phase, which led to an anharmonic coefficient $w_a = 22 \text{ cm}^{-1}$. We then considered the low-temperature ordered monolayer of CO molecules adsorbed on MgO(001). When the sole anharmonicity of the potential of the in-phase stretching mode is considered, an anharmonic coefficient $w_a = 10 \text{ cm}^{-1}$ is obtained, which decreases to $w_a = 0.7 \text{ cm}^{-1}$ when phonon-phonon couplings are explicitly taken into account among all of the six CO stretching modes of the $c(4 \times 2)$ ordered phase (three of which are infrared active). These findings are summarized in Table 1. Therefore, the vanishing anharmonicity of the in-phase CO stretching vibration in the $c(4 \times 2)$ phase is to be understood as

Table 1 Anharmonic coefficient $w_a = 2\nu^{0-1} - \nu^{0-2}$ (in cm^{-1}) of the stretching mode of CO in gas phase and in the low-temperature ordered $c(4 \times 2)$ monolayer adsorbed on MgO(001) surfaces

	Calc.	Exp.
Gas phase CO	22	26
$c(4 \times 2)$ CO MgO(001)	1	0

a global effect in the CO monolayer where lateral interactions and couplings among collective vibrations play a key role.

Conflicts of interest

There are no conflicts to declare.

Acknowledgements

J. M. and A. E. thank the University of Torino and the Compagnia di San Paolo for funding (CSTO169372).

Notes and references

- G. Pacchioni, G. Cogliandro and P. S. Bagus, *Surf. Sci.*, 1991, 255, 344–354.
- G. Pacchioni, G. Cogliandro and P. S. Bagus, *Int. J. Quantum Chem.*, 1992, 42, 1115–1139.
- K. M. Neyman and N. Rösch, *Surf. Sci.*, 1993, 297, 223–234.
- M. A. Nygren, L. G. M. Pettersson, Z. Barandiarán and L. Seijo, *J. Chem. Phys.*, 1994, 100, 2010–2018.
- K. M. Neyman, S. P. Ruzankin and N. Rösch, *Chem. Phys. Lett.*, 1995, 246, 546–554.
- M. A. Nygren and L. G. Pettersson, *J. Chem. Phys.*, 1996, 105, 9339–9348.
- G. Pacchioni, *Surf. Rev. Lett.*, 2000, 7, 277–306.
- G. Spoto, E. N. Gribov, G. Ricchiardi, A. Damin, D. Scarano, S. Bordiga, C. Lamberti and A. Zecchina, *Prog. Surf. Sci.*, 2004, 76, 71–146.
- M. Sterrer, T. Risse and H.-J. Freund, *Surf. Sci.*, 2005, 596, 222–228.
- C. Qin, *Chem. Phys. Lett.*, 2008, 460, 457–460.
- R. Valero, J. R. Gomes, D. G. Truhlar and F. Illas, *J. Chem. Phys.*, 2008, 129, 124710.
- B. Civalleri, L. Maschio, P. Ugliengo and C. M. Zicovich-Wilson, *Phys. Chem. Chem. Phys.*, 2010, 12, 6382–6386.
- A. D. Boese and J. Sauer, *Phys. Chem. Chem. Phys.*, 2013, 15, 16481–16493.
- M. Alessio, D. Usvyat and J. Sauer, *J. Chem. Theory Comput.*, 2018, 15, 1329–1344.
- V. Panella, J. Suzanne, P. N. M. Hoang and C. Girardet, *J. Phys. I*, 1994, 4, 905–920.
- R. Gerlach, A. Glebov, G. Lange, J. Toennies and H. Weiss, *Surf. Sci.*, 1995, 331–333, 1490–1495.
- J. Heidberg, M. Kandel, D. Meine and U. Wildt, *Surf. Sci.*, 1995, 331–333, 1467–1472.
- P. Hoang, S. Picaud and C. Girardet, *Surf. Sci.*, 1996, 360, 261–270.
- C. Minot, M. A. Van Hove and J.-P. Biberian, *Surf. Sci.*, 1996, 346, 283–293.
- C. Girardet, P. N. M. Hoang and S. Picaud, *Phys. Rev. B: Condens. Matter Mater. Phys.*, 1996, 53, 16615–16620.
- A. K. Sallabi and D. B. Jack, *J. Chem. Phys.*, 2000, 112, 5133–5143.
- B. Demirdjian, D. Ferry, J. Suzanne, P. N. M. Hoang, S. Picaud and C. Girardet, *Surf. Sci.*, 2001, 494, 206–212.

- 23 A. Erba, J. Maul, M. Ferrabone, P. Carbonnière, M. Rérat and R. Dovesi, *J. Chem. Theory Comput.*, 2019, 15, 3755–3765.
- 24 A. Erba, J. Maul, M. Ferrabone, R. Dovesi, M. Rérat and P. Carbonnière, *J. Chem. Theory Comput.*, 2019, 15, 3766–3777.
- 25 R. Dovesi, A. Erba, R. Orlando, C. M. Zicovich-Wilson, B. Civalleri, L. Maschio, M. Rérat, S. Casassa, J. Baima, S. Salustro and B. Kirtman, *Wiley Interdiscip. Rev.: Comput. Mol. Sci.*, 2018, 8, e1360.
- 26 A. Erba, J. Baima, I. Bush, R. Orlando and R. Dovesi, *J. Chem. Theory Comput.*, 2017, 13, 5019–5027.
- 27 R. Dovesi, R. Orlando, A. Erba, C. M. Zicovich-Wilson, B. Civalleri, S. Casassa, L. Maschio, M. Ferrabone, M. De La Pierre, P. D'Arco, Y. Noël, M. Causá, M. Rérat and B. Kirtman, *Int. J. Quantum Chem.*, 2014, 114, 1287–1317.
- 28 M. F. Peintinger, D. V. Oliveira and T. Bredow, *J. Comput. Chem.*, 2013, 34, 451–459.
- 29 T. H. Dunning, *J. Chem. Phys.*, 1989, 90, 1007–1023.
- 30 L. Mino, G. Spoto, S. Bordiga and A. Zecchina, *J. Phys. Chem. C*, 2012, 116, 17008–17018.
- 31 L. Mino, G. Spoto, S. Bordiga and A. Zecchina, *J. Phys. Chem. C*, 2013, 117, 11186–11196.
- 32 A. Erba, D. Caglioti, C. M. Zicovich-Wilson and R. Dovesi, *J. Comput. Chem.*, 2017, 38, 257–264.
- 33 N. Mina-Camilde, I. C. Manzanares and J. F. Caballero, *J. Chem. Educ.*, 1996, 73, 804.